Talanta 232 (2021) 122416

Contents lists available at ScienceDirect

Talanta

journal homepage: www.elsevier.com/locate/talanta

FeS_2 nanoparticles decorated carbonized Luffa cylindrica as biofilm substrates for fabricating high performance biosensors

Ling Liu [a,b,c], Liang Huang [b], Dengbin Yu [a,b,c], Guangxin Zhang [a,c,**], Shaojun Dong [b,c,*]

[a] Northeast Institute of Geography and Agroecology, Chinese Academy of Sciences, The High-tech North District, 4888 Sheng Bei Street, Changchun, 130102, PR China
[b] State Key Laboratory of Electroanalytical Chemistry, Changchun Institute of Applied Chemistry, Chinese Academy of Sciences, Changchun, 130022, PR China
[c] University of the Chinese Academy of Sciences, Beijing, 100049, PR China

ARTICLE INFO

Keywords:
Biosensor
Biofilm
Biomass
LIVE/DEAD assay
Toxicity assay
High-throughput sequencing

ABSTRACT

A high-performance microbial biosensor was fabricated with a reasonably designed biofilm substrate, where the aerogel of carbonized *Luffa cylindrica* (LC) was used as the scaffold for loading biofilm and FeS_2 nanoparticles (FeS_2NPs) were employed to modify this aerogel (FeS_2NPs/Gel_{LC}). The fabricated FeS_2NPs/Gel_{LC} exhibited a spring-like structure similar with that of the raw LC, which facilitated the linkage of the scaffold and promoted its mechanical strength, and further prolonged the service period of the as-prepared biosensor from few days to two months. Meanwhile, the introduced FeS_2NPs improved the microbial electron transfer of the biofilm and causing an increase in the sensor's signals from 155.0 ± 2.6 to 352.0 ± 17.1 nA and a decrease in the detection limit from 0.95 to 0.38 mg O L^{-1} (S/N = 3) for the detection of glucose-glutamic acid (GGA). More important, the FeS_2NPs had been demonstrated to have the capability for modulating a persistent shift of the microbial community with organic pollutant biodegradability. Compared with the Gel_{LC}, the FeS_2NPs/Gel_{LC} exhibited a promising performance for measuring the synthetic sewage and real water samples in BOD assay and an increasing inhibition-ratio for detecting 3,5-dichlorophenol (DCP) in toxicity assay. Based on the vast resource and renewability of LC, this work pave a new avenue for developing high-performance microbial biosensors that are expected to be the engineering production.

1. Introduction

Microbial sensor is widely used for detecting water contaminations, and the microbes are usually fixed on a substrate to form a biofilm-based device, where the microbial cells mostly undergo an unnatural environment [1,2]. The substrate that serves as the habitat for microbes mainly determines the biofilm's properties as well as the biosensor's performances. Generally, two aspects of the substrate can affect the properties of the biofilm. Firstly, for using as the scaffold to load and support the biofilm, the chemical structure of the substrate should be mechanically and chemically stable for a long term usage, porous for providing large surface area and facilitating substance diffusion, biocompatible to the microbial activity, and readily available for the batch production in the industry. Secondly, the surface functionality of the substrate directly regulates the microbial adhesion, proliferation, colonization, and metabolic activity, which can be enhanced by various modified approaches [3]. So far, a wide range of substrate have been developed for the microbial immobilization, and they mostly suffer from the issues of relatively invalid microbial adhesion, weak activity of attached biofilm, poor substance transport, resulting in the restriction of the biosensors' applications in the practice [4]. Therefore, it is highly desirable to develop new substrate for promoting the performance of microbial sensors.

In recent years, a sustained interest has been inspired by using the 3D carbonaceous materials (3DCMs) as the biofilm substrates due to their high surface area, good stability and decent biocompatibility [5–7]. 3DCMs can be prepared by chemical synthesis or carbonizing biomass related derivatives [8]. The synthesized 3DCMs generally get involved with some harsh reaction processes, such as high temperature or a large amount of chemical agents (e.g., strong acids and bases) that are energy

* Corresponding author. State Key Laboratory of Electroanalytical Chemistry, Changchun Institute of Applied Chemistry, Chinese Academy of Sciences, Changchun, 130022, PR China.
** Corresponding author. Northeast Institute of Geography and Agroecology, Chinese Academy of Sciences, The High-tech North District, 4888 Sheng Bei Street, Changchun, 130102, PR China.
E-mail addresses: zhgx@iga.ac.cn (G. Zhang), dongsj@ciac.ac.cn (S. Dong).

https://doi.org/10.1016/j.talanta.2021.122416
Received 12 February 2021; Received in revised form 29 March 2021; Accepted 7 April 2021
Available online 19 April 2021
0039-9140/© 2021 Elsevier B.V. All rights reserved.

consumption and not environmentally friendly. The prepared polymeric materials usually have a closed embedding structure that restrict the diffusion of the aqueous medium. In contrast, the biomass-based materials are generally produced by the carbonization of crude biomass materials under a facile and benign condition, such as hydrothermal carbonization [3]. Especially for those plant-derived biomass materials, they are more suitable for using as the scaffold to load biofilm due to the microcellular unit of their vascular bundle architecture [9–11]. Thus, a lot of plant-derived materials have been developed as the biofilm substrates, including wood, coal, coke, nutshell, and so forth [12,13]. Those plant resources are extensive and renewable, which is an attractive trait from the engineering perspective [14].

Modification of the substrate has proved to be an efficient way for enhancing the performance of the fabricated biosensors, and three classes of the modified materials have been reported by previous works [15,16]: 1) carbon-based materials, such as carbon nanotubes [17]; 2) metal/metal oxide-based materials, such as FeS_2 and platinum [18]; 3) conducting polymers, such as polyaniline [19]. Among them, FeS_2 is found to possess attractive characteristics for modifying the substrate of biofilm [20]. FeS_2 can mediate the electron-transfer for many dissimilatory metal-reducing bacteria, who use Fe(III) as the electron acceptors [21], while elemental sulfur can also mediate electron-shuttling during bacterial iron reduction [22]. Moreover, it is easy to prepare FeS_2 that is important for further industrial production [23].

In this work, we reported the fabrication of a new biofilm substrate by carbonizing the fruit of a plant of the genus Luffa (*Luffa cylindrica*, not the loofah sponge) as the scaffold and decorating FeS_2NPs simultaneously. A wide range of characterization techniques have been employed to investigate the structures and the properties of FeS_2NPs/Gel_{LC} aerogel. The microbial community structures in the biofilm were studied by high-throughput sequencing (HTS). Particularly, the resultant FeS_2NPs/Gel_{LC} aerogel-based microbial biosensors exhibited a high performance for the detection of water contaminations, such as biochemical oxygen demand [13] and water total toxicity (WTT).

2. Experimental

2.1. Materials

Graphite was purchased from Alfa Aesar. $FeCl_3$, $(NH_2)_2CS$, urea, NaCl, $K_2HPO_4{\cdot}3H_2O$, $CaCl_2{\cdot}2H_2O$, $MgSO_4{\cdot}7H_2O$, $Na_2HPO_4{\cdot}12H_2O$, KH_2PO_4, KCl, glucose and glutamic acid were purchased from Beijing Chemical Factory (Beijing, China). Peptone and beef extract were OXOID products. All of the raw biomass materials were obtained from a local supermarket and thoroughly washed by sterile water prior to usage. All of other reagents were of analytical grade and used as received. The ultrapure water (>18 MΩ) from a Milli-Q Plus system (Millipore) were used for preparing aqueous solutions unless otherwise stated. The phosphate buffer (PB, pH 7) solution was comprised of 0.12 M Na_2HPO_4, 0.08 M KH_2PO_4 and 0.1 M KCl.

2.2. Preparation of the biofilm substrate

A series of carbonized biomass materials, including fresh LC, loofah sponge, tea hybridized with sodium alginate (denoted as tea-alg), scallion stalk, Chinese cabbage, orange peel and onion were tested and compared in this work and they were treated by a similar condition of hydrothermal method. In a typical preparation procedure, a crude biomass material was cut into about 0.5 cm^3 block. 20 mL of modified solution composed of 10 mL 0.225 g mL^{-1} $FeCl_3$, 10 mL 0.038 g mL^{-1} $(NH_2)_2CS$, and 50 μL 28% ammonia was added to immerse the block of plant in a Teflon-lined autoclave. The mixture solution was heated at 180 °C for 8 h to form the carbonized biomass-based material with the FeS_2NPs decorated on it. Then the autoclave was cooled to room temperature naturally, and the as-prepared hydrogel was picked out and washed thoroughly with deionized water. For the aerogel preparation, the as-prepared biomass-based material was freeze-dried to remove absorbed water. As for comparison, a same plant block was prepared by the similar treated condition but adding of 20 mL ultrapure water to replace the modified solutions. The reduced graphene oxide aerogel (Gel_{rGO}) was prepared according to our previous report [24].

2.3. Preparation of biofilm and biosensor

The biosensor driven by a flow system was fabricated according to Scheme S1. The measurements were performed with a CHI 832 electrochemical workstation (CH Instruments, Inc., China). The biofilm therein was cultured by a laboratory-scale process that was continuously fed with LB medium diluted 10 times by PB solution. The controlled conditions were carried out with a flow rate of 3 mL min^{-1} at 35 °C for over 48 h. The tested solutions, glucose and glutamic acid (GGA) stock and OECD stock, were prepared according to Table S1. The real water samples were obtained from a local lake, Chagan. The measured endpoint of the biosensor was the current signal recorded by the electrochemical workstation under i-t curve mode at the Au working electrode. The changes of the current signals were caused by the fluctuation of dissolved oxygen (DO), which was the electron acceptor of the microbial respiration.

2.4. Microbial morphologies and LIVE/DEAD assay

The microbial cell viabilities were analyzed with the LIVE/DEAD BacLight bacterial viability kit (No. L13152). The staining procedure was conducted according to the manufacturer's instruction. Confocal laser scanning microscopy (CLSM, Nikon, C2, Japan) was used to image the microbial morphologies and structures of the biofilm. The ultrathin sections (Leica UC 6 microtome, Leica, Austria) of microbial cells, transmission electron microscopy (TEM, H-7650 TEM, Hitachi, Japan) and scanning electron microscope (SEM, XL30 ESEM, Philip, Holland) analyses were operated according to our previous report [25]. The high-resolution TEM (HRTEM) images were obtained with a JEM-2010 apparatus operating at 200 kV, equipped with an energy-dispersive spectrometer (EDS).

2.5. Microbial communities in the biofilms

Before and after operations of the biosensor, a piece of the biofilm was cut and picked out for microbial community analysis by HTS technique. A detailed description of the total DNA extraction, polymerase chain reaction (PCR) amplification reaction, 16S rRNA gene amplification, sequencing, and data processing were mainly referenced the previous study [26–28]. Specifically, PCRs were run on an ABI GeneAmp-9700 PCR instrument. KAPA HiFi Hot start DNA Polymerase (Kapa Biosystem KE2501) was used for amplifying. Amplicons were extracted from 2% agarose gels and purified using an AMPure XP Beads (Beckman Coulter). The DNA samples were stored at −20 °C and analyzed within 3 months. Illumina HTS was performed on a NovaSeq platform (Illumina, USA). The raw reads were demultiplexed and quality-filtered by using QIIME (v1.9.1) [29].

3. Results and discussion

3.1. Characterization of the FeS_2NPs/Gel_{LC}

The structures of as-prepared aerogel were first characterized by SEM. As shown in Fig. 1a, the original frameworks with sheet and spongy shapes of the LC were remained and further interconnected into a continuous 3D macroporous structure with the pore diameters of 10–50 μm, which was a favorable space for loading microbial biofilm and facilitating the diffusion of aqueous medium. After the modification by FeS_2NPs, the material morphologies were kept well (Fig. 1b). Since the FeS_2NPs could not been clearly imaged by SEM, all of the materials

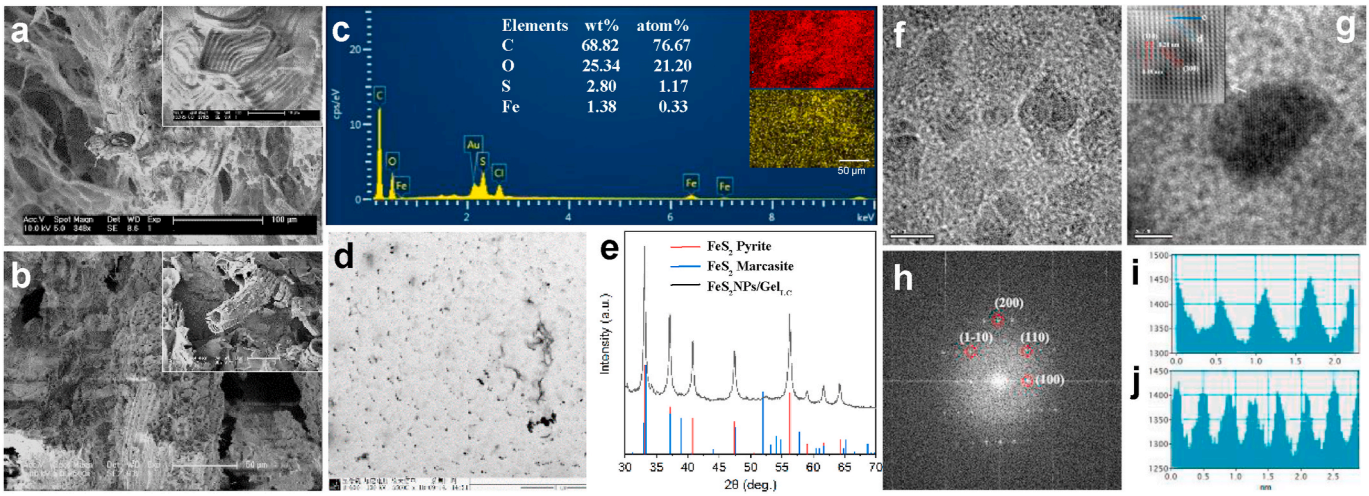

Fig. 1. Morphological and structural characterizations of Gel_{LC}. Representative SEM images for Gel_{LC} (a) and FeS_2NPs/Gel_{LC} (b). Insets, amplifications for exhibiting the special structures. EDS spectra (c). Inset, the corresponding elemental contents and elemental mapping images for S and Fe. TEM images (d) and XRD pattern (e) of FeS_2NPs/Gel_{LC}. HRTEM images and lattice spacing of the FeS_2NPs (f and g). Corresponding FFT pattern (h) and lattice spacing (i and j).

with FeS_2NPs were therefore imaged by TEM in the following work. In the EDS pattern of FeS_2NPs/Gel_{LC} (Fig. 1c), the aerogel mainly contained C and O with the atom percent of 76.67% and 21.20% (inset in Fig. 1c), respectively, indicating a high carbonization degree of the as-prepared material. Beyond that, the elements of Fe and S were also observed in the EDS spectra. In Fig. 1d, the TEM image shown that the FeS_2NPs were uniformly deposited on the Gel_{LC} scaffold. The characteristic XRD pattern (Fig. 1e and an only Gel_{LC} pattern in Figure S1) further indicated that the synthesized FeS_2 possessed a single-phase marcasite [30]. HRTEM images (Fig. 1f–j) exhibited that the FeS_2NPs

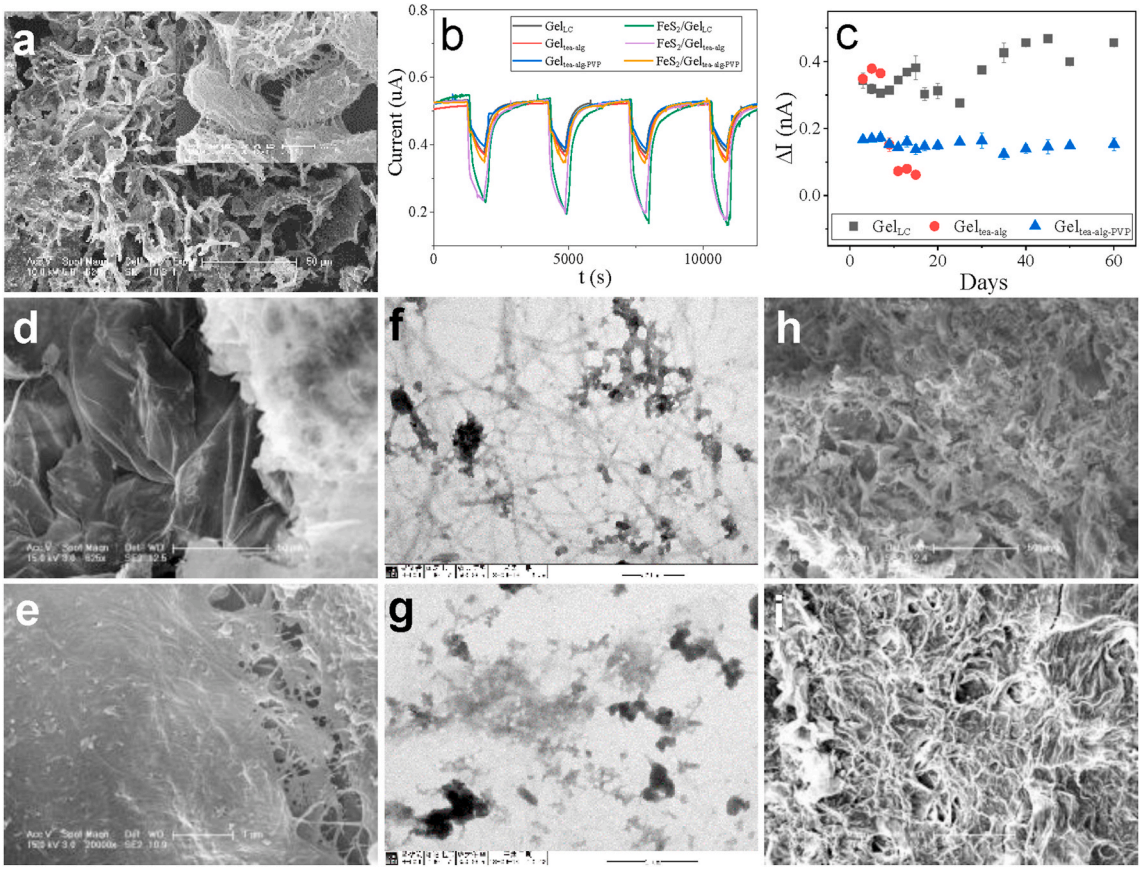

Fig. 2. SEM images of the microbes deposited on the FeS_2NPs/Gel_{LC} (a). Inset, amplification for exhibiting the special structures. I-t current signals for measuring GGA20 solution (b) by the biosensors based on, Gel_{LC}, FeS_2NPs/Gel_{LC}, $Gel_{tea\text{-}alg}$ (red), $FeS_2NPs/Gel_{tea\text{-}alg}$ (purple), $Gel_{tea\text{-}alg\text{-}PVA\text{-}g\text{-}4VP}$ (blue) and $FeS_2NPs/Gel_{tea\text{-}alg\text{-}PVA\text{-}g\text{-}4VP}$ (yellow) biofilms. The service period of the biosensors based on FeS_2NPs/Gel_{LC}, $FeS_2NPs/Gel_{tea\text{-}alg}$ (red) and $FeS_2NPs/Gel_{tea\text{-}alg\text{-}PVA\text{-}g\text{-}4VP}$ (blue) (c). SEM images of $Gel_{tea\text{-}alg}$ (d) and $Gel_{tea\text{-}alg\text{-}PVA\text{-}g\text{-}4VP}$ (e). TEM images of $FeS_2NPs/Gel_{tea\text{-}alg}$ (f) and $FeS_2NPs/Gel_{tea\text{-}alg\text{-}PVA\text{-}g\text{-}4VP}$ (g), and the corresponding biofilm SEM images (h) and (i). GGA20, 20 mg L^{-1} of BOD value for the GGA solution. (For interpretation of the references to colour in this figure legend, the reader is referred to the Web version of this article.)

were 5–10 nm and the crystal lattice spacing values were 0.28 nm and 0.38 nm corresponded to the (110) and (200) planes of the FeS_2 [31]. The present results indicated that the FeS_2NPs/Gel_{LC} had been successfully prepared. The uniform morphologies and sizes of the FeS_2NPs were helpful for their reproducible properties in the engineering production [20]. Furthermore, to evaluate the biocompatibility of this aerogel, the microbes freshly cultured by flask were directly dropped onto the FeS_2NPs/Gel_{LC} and their morphologies were kept well (Fig. 2a). Beyond that, some wire-like structures of the deposited microbes were observed (inset in Fig. 2a), which appeared like the microbial nanowires (or pili) or likely formed by some extracellular substances [32]. Nevertheless, these structures were useful for tethering the microbial cells to the surface of substrate, and thereby helpful for the biofilm formation in the subsequent steps.

3.2. Rationality for Gel_{LC} as the biofilm scaffold

Before adopting Gel_{LC} as the scaffold material, a series of other blocky plants were actually compared to prepare aerogel materials and used as the microbial substrate (Table S2). The criterion for choosing these materials was economic, cellulose-rich and blocky. Besides, graphene oxide (GO) was also employed because of the widespread attention paid to it and its derivatives. These materials were treated by the same procedures of the carbonization and characterization for Gel_{LC} (Figure S2) and their properties were listed in Table 1. Obviously, the properties of Gel_{LC} and $Gel_{tea\text{-}alg}$ were better than the others for fabricating the biosensor with a very small chamber, about 0.5 cm^3 in this work, which was useful for measuring the samples with a small amount. Herein, the biosensor was used for detecting water contaminations, including BOD and WTT. The detail measuring and calculating procedures were shown in Scheme S1. The relationship between the microbial morphologies of the biofilms and the net current (ΔI) of the measured signals by the biosensors were studied (Fig. 2b). After modifying by FeS_2NPs, the ΔIs obtained by Gel_{LC} biosensor and $Gel_{tea\text{-}alg}$ biosensor were increased from 155.0 ± 2.6 nA to 352.0 ± 17.1 nA and from 171.3 ± 6.4 nA to 339.9 ± 12.5 nA, respectively, implying the FeS_2NPs was helpful for the electron transfer of the biosensor. A linear detection range of 2–30 mg O L^{-1} can be deduced for detecting GGA standard solutions of BOD by both biofilm with a detection limit of 0.38 and 0.95 mg O L^{-1} (S/N = 3) for FeS_2NPs/Gel_{LC} and Gel_{LC} biofilm, respectively. However, the signals by the $Gel_{tea\text{-}alg}$ biosensor was sharply decreased in a few days (Fig. 2c). By checking the biosensor, it was found that the $Gel_{tea\text{-}alg}$ substrate was dispersed into some fragments and lost via the flow system (Figure S3). To elucidate the reason for that, the distinct structures of these two materials were compared and some spring-like architectures were observed for the Gel_{LC} SEM images (inset in Fig. 1a). These structures could be destroyed under the harsh prepared conditions (Figure S4), and resulting in a low mechanical strength of the resultant carbonized material, indicating the spring-like structures might act the linking and supporting functions for keeping the Gel_{LC} frameworks. To confirm that, the copolymer of poly(vinyl alcohol-g-4-vinylpyridine) (PVA-g-4VP), that had the similar linking function due to its grafted long chain, was employed to improve the interconnection of $Gel_{tea\text{-}alg}$ (to form the $Gel_{tea\text{-}alg\text{-}PVA\text{-}g\text{-}4VP}$). By comparing Fig. 2d and e, the interconnections of the aerogel $Gel_{tea\text{-}alg\text{-}PVA\text{-}g\text{-}4VP}$ were more tightly than that of $Gel_{tea\text{-}alg}$, and the activity of the biosensor had been prolonged to 2 months (Fig. 2c). But the current signals were actually reduced from about 400 nA to 180 nA in the wake of hybridization with PVP, despite the FeS_2NPs had been deposited on the material (Fig. 2f and g) and the biofilms had also been successfully cultured (Fig. 2h and i). The properties of the Gel_{LC}, $Gel_{tea\text{-}alg}$ and their derivatives were summarized in Table 2, and it was clear that FeS_2NPs/Gel_{LC} was the best. Combining these results together, the Gel_{LC} was better than the other tested materials used as the scaffold for fabricating biosensor in this work and the its spring-like structures were beneficial for keeping its mechanical strength in the long term service period of the biosensor.

Table 1
The properties of different materials were compared for loading of biofilm and fabricating of biosensor.

Raw materials	Formation of aerogel	Install in biosensor	Microbial mass in biofilm	Diffusion of aqueous medium ([b])
onion	No	–	–	–
loofah sponge	Yes	no([a])	–	–
scallion stalk	Yes	yes	Low	–
cabbage	yes	yes	Low	–
orange peel	yes	yes	Low	–
Gel_{rGO}	yes	yes	High	bad
tea-alg	yes	yes	High	good
LC	yes	yes	High	good

[a] The material was broken by cutting into 0.5 cm^3 block to match the chamber of the sensor.
[b] The diffusion of aqueous medium was evaluated by the amount of the water flowed through the sensor and the two materials with the highest water volume were signed as good. -, no.

3.3. Functions of the modified material FeS_2NPs

Furthermore, the reason for the high performance of the FeS_2NPs modified substrate was explored by a multistep analysis. First of all, the microbial masses loaded on the substrates were weighed, and 25 mg cm^{-3} and 20 mg cm^{-3} were obtained for Gel_{LC} and FeS_2NPs/Gel_{LC}, respectively (Table 2 and Fig. 3a), suggesting that the adhesion of microbes on the substrate was slightly inhibited upon forming FeS_2NPs. However, we note that the current signals obtained by the FeS_2NPs/Gel_{LC} biosensor was higher than that by Gel_{LC} only. Thus, the microbial activities in the biofilms were examined via the LIVE/DEAD assay characterized by CLSM, where SYTO9 was used for staining the live cells and PI for the compromised cells. As shown in Fig. 3b and c, the microbes in the FeS_2NPs/Gel_{LC} biofilm stained by PI were over 90%, while about 85% for Gel_{LC}, indicating the microbes in the both biofilms were almost sacrificed, however, both two biosensors still exhibited significant signals for measuring organic substances. By combining the results in these two experiments, there were two issues were needed to be explained: a) The PI stained ratio and the current signals measured by the two biosensors were contradictory. b) The biofilm property on Gel_{LC} seemed better than that on FeS_2NPs/Gel_{LC}, but in contrast, the performance of FeS_2NPs/Gel_{LC} biosensor was better.

To discuss the issue a), the ultrathin sections of the microbes in these biofilms were imaged by TEM. Comparing with the freshly cultured

Table 2
The properties of the substrates by carbonizing of the LC, tea-alg and their derivatives.

Materials	Properties of materials		Properties of microbes or biofilms		
	Stability in this work[a]	Microbial masses (mg cm^{-3})	PI %	Current signals ΔI (nA)	Service period (days)
$Gel_{tea\text{-}alg}$	good	20 ± 5	85	120	10
FeS_2NPs/$Gel_{tea\text{-}alg}$	good	20 ± 5	85	400	60
FeS_2NPs/$Gel_{tea\text{-}alg\text{-}PVA\text{-}g\text{-}4VP}$	good	5 ± 5	85	180	60
Gel_{LC}	good	25 ± 5	85	120	60
FeS_2NPs/Gel_{LC}	good	20 ± 5	90	400	60

[a] The stability of a material was defined by checking the state after a week of test period. If a material was intact and not broken, its stability was good.

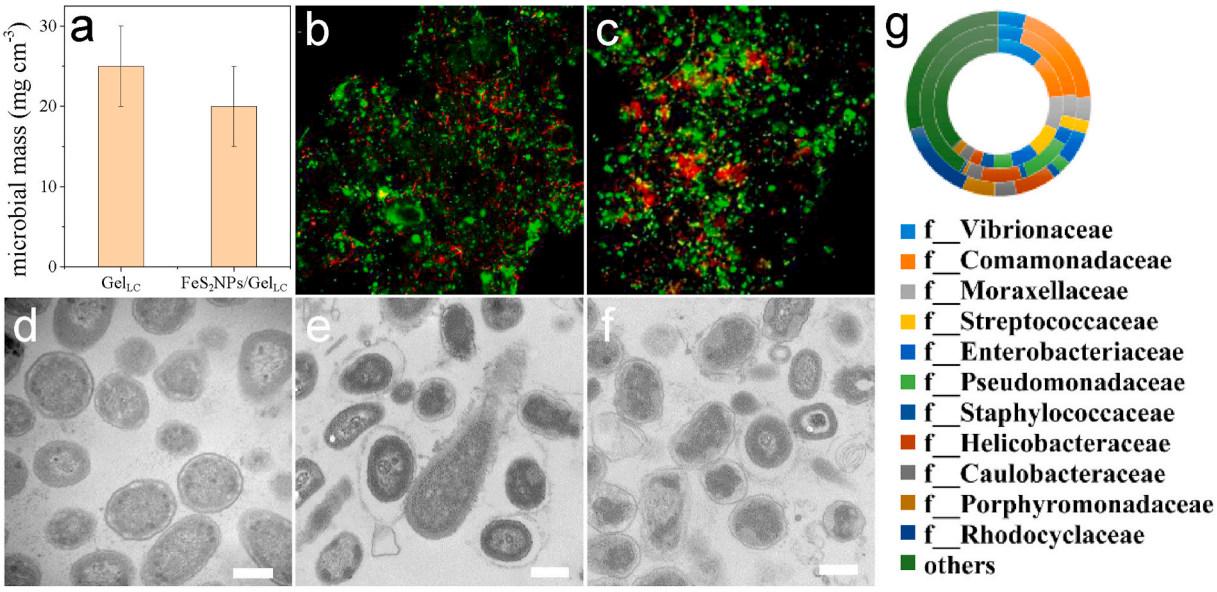

Fig. 3. Microbial mass loaded on the Gel_{LC} and on the FeS_2NPs/Gel_{LC} (a). CLSM images for the Gel_{LC} biofilm (b) and FeS_2NPs/Gel_{LC} biofilm (c). TEM images of the refresh cultured microbes (d), the microbes from Gel_{LC} biofilm (e) and FeS_2NPs/Gel_{LC} biofilm (f). Relative abundances of major bacterial groups at family levels with sequence percentage >1% (g), from inner ring to outer ring were real water sample, the biofilms on Gel_{LC} and FeS_2NPs/Gel_{LC} for measuring the water two weeks.

microbes (Fig. 3d), the microbial cells in the both biofilms were changed seriously (Fig. 3e and f). The CLSM results indicated that all of the microbes in the present biofilms were "death" or "near-death". These results were just same with that reported by our previous work that these microbes had got a viable but with PI permeable membranes state, which was neither live nor death, but between them, and it was beneficial for long term application of the biosensor [25]. Additionally, in the CLSM images, the microbial cells had no a hard edge due to that it was surrounded by some extracellular polymeric substances (EPS) [33]. It was a fundamental component and determined the physiochemical properties of the biofilm, because the redox molecules from the tested solutions could diffuse in the EPS and were involved in transferring electrons between cells and electron donors/acceptors, and thus leading to an enhanced current signals [32]. Prudently, the electron transfer across the biological and non-biological interfaces was complex and more deep evidences should be explored and discussed in the future.

Herein, to understand the reason for the performance of FeS_2NPs/Gel_{LC} biosensor better than that of Gel_{LC} (the issue b mentioned above), the microbial communities and their functions in the biofilms were analyzed by gene sequencing technique. The dominated phyla were commonly environmental microbes and without significant distinctions between the three samples, a real water sample (signed as B), and the biofilms in Gel_{LC} or FeS_2NPs/Gel_{LC} sensors for measuring the water two weeks (Figure S5). Then, the class level was analyzed, the OTUs belonging to *Proteobacteria* (34.6%), *Bacilli* (16.7%), *Deltaproteobacteria* (14.2%) and *Betaproteobacteria* (12.0%) in the sample B were almost remained in the Gel_{LC} biofilm as 25.4%, 5.9%, 29.1% and 18.8%, respectively, and were changed in the FeS_2NPs/Gel_{LC} biofilm as that *Betaproteobacteria* had increased 33.9% (Figure S6). This class included the groups of Gram-negative aerobic or facultative bacteria that often have versatile degradation capacities [34,35], which could be helpful for increasing the biodegradability of the FeS_2NPs/Gel_{LC} biosensor. For the family and genus levels, the sequences with more than 1% were organized into a circle diagram in Fig. 3g. Family *Vibrionaceae* and genus *Vibrio* were significantly reduced in the process of the sensor operation. These microbes had been used as the biocontrol agents or the living antibiotics against harmful bacteria in the aquaculture industry due to their unique bactericidal ability [36,37], which was accordant with the fishing function of Chagan Lake. These species were primarily a result of the bio-addiction in the industry and could not be sustainably kept, and thus they were lost in the operated period [38]. Additionally, the family *Rhodocyclaceae* was significantly enhanced with the operation process of the FeS_2NPs/Gel_{LC} sensor. This result indicated that *Rhodocyclaceae* might play an important role in pyrite-oxidizing denitrification, which was similar as the previous report that *Rhodococcus* excreted the menaquinone-related electron shuttles and facilitated for electron transfer [34,39]. Moreover, the species *Helicobacteraceae* and *Porphyromonadaceae* had been reported to have more activity for degrading organic matter [40], which were also annotated with an increased trend in the FeS_2NPs/Gel_{LC} biofilm. The present results indicated that the microbial community structure was a key factor for impacting the performance of the as-prepared biosensor and the communities in the FeS_2NPs/Gel_{LC} biofilm were more suitable for degradation of organic substances.

3.4. Applications of the FeS_2NPs/Gel_{LC} biosensor

The increase of the microbes for nitrogen transformation is conducive to the degradation of N-containing compounds, which is more useful to reflect the real contamination of water samples. Herein, a biofilm reactor based on Gel_{LC} or FeS_2NPs/Gel_{LC} was then integrated into a BOD instrument developed by our group and commercialized by our cooperative partner (detail in Figure S7). The Organisation for Economic Cooperation and Development [41] synthetic sewage feed (Table S1) that had more complex components than GGA and highly biology difficult to be degraded was measured by the present sensor. As shown in Fig. 4a, the results obtained by FeS_2NPs/Gel_{LC} sensor was obviously better than that by Gel_{LC} sensor, and the slope of the linear fitting equations was increased from 4.2 to 14.9 μA/mg L^{-1}, it was benefit by the large current measured by the FeS_2NPs/Gel_{LC} biofilm. Beyond that, the large current measured signal was also helpful for the sensitive detection of some toxic substances. For example, the inhibition ratio for detecting of DCP was increased from 18.6% by the Gel_{LC} sensor to 57.9% by the FeS_2NPs/Gel_{LC} sensor (Fig. 4b, inhibition calculation Eq. S1). Additionally, for measuring the real samples from a local lake (Chagan Lake), the current signals by FeS_2NPs/Gel_{LC} biosensor shown a fitted results with the standard 5-days method (Pearson's coefficient 0.9985 and $R^2 = 0.996$ in Fig. 4c). The present results indicated that the FeS_2NPs/Gel_{LC} biofilm was fully competent for the practical usages and the biosensor had high performances.

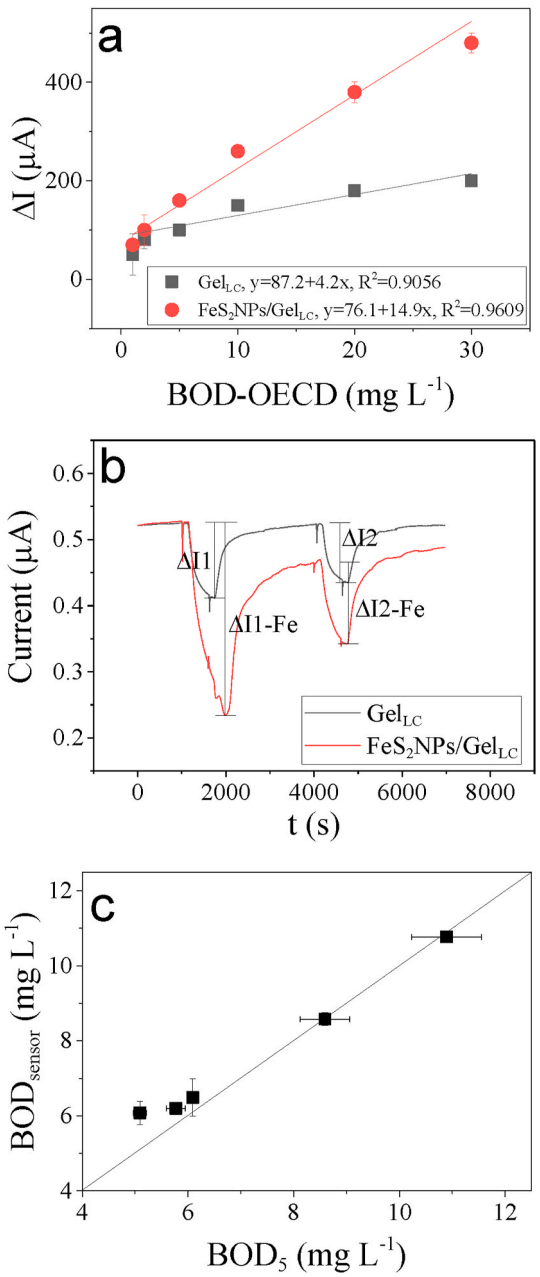

Fig. 4. Detection of OECD solutions by the Gel_{LC} biosensor (black squares) and the FeS_2NPs/Gel_{LC} biosensor (red dots) in (a). I-t current signals for detecting 10 mg L^{-1} DCP by the Gel_{LC} biosensor (black curve) and the FeS_2NPs/Gel_{LC} biosensor (red curve) in (b). Measuring the real sample from the Chagan Lake compared with the standard BOD_5 method (c). (For interpretation of the references to colour in this figure legend, the reader is referred to the Web version of this article.)

4. Conclusions

A high performance biosensor for measuring water contaminants was fabricated by employing FeS_2NPs/Gel_{LC} as the substrate of biofilm. The marrying FeS_2NPs with Gel_{LC} in the form of a composite offered a series of benefit in terms of the following, Gel_{LC} was an ideal candidate used as the scaffold to load and support a biofilm. 1) It was a fibrous matrices with the inherent void volume, permeability and low cost that make it particularly attractive. The carbonized process was nearly green synthesis. 2) The special spring-like structure of Gel_{LC} had been demonstrated to play the linking and supporting acts for it used as the scaffold of biofilm.

FeS_2NPs had two functions in the present work. 1) It externally improved the microbial electron transfer of the biofilm and thereby enhanced its metabolic activity for catalyzing the organic matter as well as the performance of as-prepared biosensor. The high activity state of the biofilm was more sensitive toward the additionally toxic chemicals, which was benefit for the toxicity assay (or risk assessment) in the environmental field. 2) It had the impact on the microbial community structure and made it more suitable for reflecting the real contamination of water samples. Our work paved the key step for developing high-performance, tractable and ultimately engineering biosensor for practical application.

Credit roles

Ling Liu, Conceptualization, Methodology, Writing-Original draft preparation. Liang Huang, Visualization, Formal analysis. Dengbin Yu, Investigation, Validation. Guangxin Zhang, Supervision. Shaojun Dong, Supervision, Project administration.

Declaration of competing interest

The authors declare that they have no known competing financial interests or personal relationships that could have appeared to influence the work reported in this paper.

Acknowledgements

This work was supported by the Jilin Province Key R&D Program of China (No. 20200403002SF), Ministry of Science and Technology of China (Nos. 2016YFA0203203, 2017YFC0406003) and the National Natural Science Foundation of China (Nos. 21675151 and 21721003).

Appendix A. Supplementary data

Supplementary data to this article can be found online at https://doi.org/10.1016/j.talanta.2021.122416.

References

[1] F. Zhao, R.C. Slade, J.R. Varcoe, Techniques for the study and development of microbial fuel cells: an electrochemical perspective, Chem. Soc. Rev. 38 (7) (2009) 1926–1939.
[2] S. Zhao, H. Yin, L. Du, L. He, K. Zhao, L. Chang, G. Yin, H. Zhao, S. Liu, Z. Tang, Carbonized nanoscale metal-organic frameworks as high performance electrocatalyst for oxygen reduction reaction, ACS Nano 8 (12) (2014) 12660–12668.
[3] Y.S. Ko, J.W. Kim, J.A. Lee, T. Han, G.B. Kim, J.E. Park, S.Y. Lee, Tools and strategies of systems metabolic engineering for the development of microbial cell factories for chemical production, Chem. Soc. Rev. 49 (14) (2020) 4615–4636.
[4] X.W. Liu, W.W. Li, H.Q. Yu, Cathodic catalysts in bioelectrochemical systems for energy recovery from wastewater, Chem. Soc. Rev. 43 (22) (2014) 7718–7745.
[5] Y. Chen, B. Dang, J. Fu, C. Wang, C. Li, Q. Sun, H. Li, Cellulose-based hybrid structural material for radiative cooling, Nano Lett. 21 (1) (2020) 397–404.
[6] H. Liu, S. Wu, N. Tian, F. Yan, C. You, Y. Yang, Carbon foams: 3D porous carbon materials holding immense potential, J. Mater. Chem. 8 (45) (2020) 23699–23723.
[7] B. Reuillard, A. Le Goff, C. Agnes, M. Holzinger, A. Zebda, C. Gondran, K. Elouarzaki, S. Cosnier, High power enzymatic biofuel cell based on naphthoquinone-mediated oxidation of glucose by glucose oxidase in a carbon nanotube 3D matrix, Phys. Chem. Chem. Phys. 15 (14) (2013) 4892–4896.
[8] X. Wang, H. Yin, G. Sheng, W. Wang, X. Zhang, Z. Lai, Fabrication of self-entangled 3D carbon nanotube networks from metal–organic frameworks for Li-ion batteries, ACS Appl Nano Mater 1 (12) (2018) 7075–7082.
[9] Y. Liu, M. Zhou, C. Jin, J. Zeng, C. Huang, Q. Song, Y. Song, Preparation of a sensor based on biomass porous carbon/covalent-organic frame composites for pesticide residues detection, Front Chem 8 (2020) 643.
[10] S. Bilge, N.K. Bakirhan, Y.O. Donar, A. Sinag, S.A. Ozkan, E.Ş. Okudan, Green synthesis of carbon based biosensor materials from algal biomass for the sensitive detection of vardenafil, J. Electroanal. Chem. 871 (2020) 114286.
[11] H. Ren, X. Liu, L. Yan, Y. Cai, C. Liu, L. Zeng, A. Liu, Ocean green tide derived hierarchical porous carbon with bi-enzyme mimic activities and their application for sensitive colorimetric and fluorescent biosensing, Sensor. Actuator. B Chem. 312 (2020) 127979.
[12] H. Zhu, X. Wang, F. Yang, X. Yang, Promising carbons for supercapacitors derived from fungi, Adv. Mater. 23 (24) (2011) 2745–2748.

[13] P.K. Kalambate, Z. Rao, Dhanjai, J. Wu, Y. Shen, R. Boddula, Y. Huang, Electrochemical (bio) sensors go green, Biosens. Bioelectron. 163 (2020) 112270.
[14] B. Thomas, M.C. Raj, A.K. B, R.M. H, J. Joy, A. Moores, G.L. Drisko, C. Sanchez, Nanocellulose, a versatile green platform: from biosources to materials and their applications, Chem. Rev. 118 (24) (2018) 11575–11625.
[15] A.A. Yaqoob, M.N.M. Ibrahim, S. Rodríguez-Couto, Development and modification of materials to build cost-effective anodes for microbial fuel cells (MFCs): an overview, Biochem. Eng. J. 164 (2020) 107779.
[16] X. Zhou, Y. Wang, C. Gong, B. Liu, G. Wei, Production, structural design, functional control, and broad applications of carbon nanofiber-based nanomaterials: a comprehensive review, Chem. Eng. J. 402 (2020) 126189.
[17] S. Matsumoto, K. Yamanaka, H. Ogikubo, H. Akasaka, N. Ohtake, Carbon nanotube dispersed conductive network for microbial fuel cells, Appl. Phys. Lett. 105 (8) (2014), 083904.
[18] S. Zhao, Y. Li, H. Yin, Z. Liu, E. Luan, F. Zhao, Z. Tang, S. Liu, Three-dimensional graphene/Pt nanoparticle composites as freestanding anode for enhancing performance of microbial fuel cells, Sci Adv 1 (10) (2015), e1500372.
[19] D.Z. Sun, Y.Y. Yu, R.R. Xie, C.L. Zhang, Y. Yang, D.D. Zhai, G. Yang, L. Liu, Y. C. Yong, In-situ growth of graphene/polyaniline for synergistic improvement of extracellular electron transfer in bioelectrochemical systems, Biosens. Bioelectron. 87 (2017) 195–202.
[20] R. Wang, M. Yan, H. Li, L. Zhang, B. Peng, J. Sun, D. Liu, S. Liu, FeS2 nanoparticles decorated graphene as microbial-fuel-cell anode achieving high power density, Adv. Mater. 30 (22) (2018), e1800618.
[21] D.R. Lovley, Dissimilatory Fe(III) and Mn(IV) reduction, Microbiol. Rev. 55 (2) (1991) 259–287.
[22] T.M. Flynn, E.J. O'Loughlin, B. Mishra, T.J. DiChristina, K.M. Kemner, Sulfur-mediated electron shuttling during bacterial iron reduction, Science 344 (6187) (2014) 1039–1042.
[23] A. Dubey, S.K. Singh, B. Tulachan, M. Roy, G. Srivastava, D. Philip, S. Sarkar, M. Das, Nano iron pyrite (FeS2) exhibits bi-functional electrode character, RSC Adv. 6 (20) (2016) 16859–16867.
[24] L. Liu, J. Zhai, C. Zhu, Y. Gao, Y. Wang, Y. Han, S. Dong, One-pot synthesis of 3-dimensional reduced graphene oxide-based hydrogel as support for microbe immobilization and BOD biosensor preparation, Biosens. Bioelectron. 63 (2015) 483–489.
[25] L. Liu, C. Liu, H. Zhang, J. He, J. Zhai, D. Yu, S. Dong, How to identify the "LIVE/DEAD" states of microbes related to biosensing, ACS Sens. 5 (1) (2020) 258–264.
[26] W. Yan, Y. Guo, Y. Xiao, S. Wang, R. Ding, J. Jiang, H. Gang, H. Wang, J. Yang, F. Zhao, The changes of bacterial communities and antibiotic resistance genes in microbial fuel cells during long-term oxytetracycline processing, Water Res. 142 (2018) 105–114.
[27] F. Peng, A. Isabwe, Y.Y. Guo, H.H. Chen, J. Yang, An extensively shared antibiotic resistome among four seasons suggests management prioritization in a subtropical riverine ecosystem, Sci. Total Environ. 673 (2019) 533–540.
[28] F. Peng, Y. Guo, A. Isabwe, H. Chen, Y. Wang, Y. Zhang, Z. Zhu, J. Yang, Urbanization drives riverine bacterial antibiotic resistome more than taxonomic community at watershed scale, Environ. Int. 137 (2020) 105524.
[29] H.J. Ding, M. Qiao, J.Y. Zhong, Y.G. Zhu, C.J. Guo, Q.Q. Zhang, P. Yang, L. Han, W. H. Zhang, Y.X. Wu, J.T. Liu, L.T. Zhang, J.H. Sun, Characterization of antibiotic resistance genes and bacterial community in selected municipal and industrial sewage treatment plants beside Poyang Lake, Water Res. 174 (2020) 115603.
[30] L. Wu, N.Y. Dzade, L. Gao, D.O. Scanlon, Z. Ozturk, N. Hollingsworth, B. M. Weckhuysen, E.J. Hensen, N.H. de Leeuw, J.P. Hofmann, Enhanced photoresponse of FeS2 films: the role of marcasite-pyrite phase junctions, Adv. Mater. 28 (43) (2016) 9602–9607.
[31] L. Zhu, B.J. Richardson, Q. Yu, Anisotropic growth of iron pyrite FeS2 nanocrystals via oriented attachment, Chem. Mater. 27 (9) (2015) 3516–3525.
[32] Y. Xiao, E. Zhang, J. Zhang, Y. Dai, Z. Yang, H.E.M. Christensen, J. Ulstrup, F. Zhao, Extracellular polymeric substances are transient media for microbial extracellular electron transfer, Sci Adv 3 (7) (2017), e1700623.
[33] Y. Xiao, F. Zhao, Electrochemical roles of extracellular polymeric substances in biofilms, Curr Opin Electroche 4 (1) (2017) 206–211.
[34] S. Jia, K. Bian, P. Shi, L. Ye, C.H. Liu, Metagenomic profiling of antibiotic resistance genes and their associations with bacterial community during multiple disinfection regimes in a full-scale drinking water treatment plant, Water Res. 176 (2020) 115721.
[35] I.A. Suvorova, M.S. Gelfand, Comparative genomic analysis of the regulation of aromatic metabolism in Betaproteobacteria, Front. Microbiol. 10 (2019) 642.
[36] K. Asmani, B. Petton, J. Le Grand, J. Mounier, R. Robert, J.-L. Nicolas, Establishment of microbiota in larval culture of Pacific oyster, Crassostrea gigas, Aquaculture 464 (2016) 434–444.
[37] J.M. Mazon-Suastegui, J.S. Salas-Leiva, R. Medina-Marrero, R. Medina-Garcia, M. Garcia-Bernal, Effect of Streptomyces probiotics on the gut microbiota of Litopenaeus vannamei challenged with Vibrio parahaemolyticus, Microbiologyopen 9 (2) (2020) e967.
[38] C. Wen, M. Xue, H. Liang, S. Zhou, Evaluating the potential of marine Bacteriovorax sp. DA5 as a biocontrol agent against vibriosis in Litopenaeus vannamei larvae, Vet. Microbiol. 173 (1–2) (2014) 84–91.
[39] J. Zhai, Z. Wang, P. Shi, C. Long, Microbial community in a biofilter for removal of low load nitrobenzene waste gas, PloS One 12 (1) (2017), e0170417.
[40] C.E. Granada, C. Hasan, M. Marder, O. Konrad, L.K. Vargas, L.M.P. Passaglia, A. Giongo, R.R. de Oliveira, L.d.M. Pereira, F. de Jesus Trindade, R.A. Sperotto, Biogas from slaughterhouse wastewater anaerobic digestion is driven by the archaeal family Methanobacteriaceae and bacterial families Porphyromonadaceae and Tissierellaceae, Renew. Energy 118 (2018) 840–846.
[41] OECD, Activated Sludge, Respiration Inhibition Test Organisation for Economic Cooperation and Development1984.